arXiv:1605.02811v2 [physics.plasm-ph] 25 Jul 2016

On the compressibility effect in test particle acceleration by magnetohydrodynamic turbulence

C.A. González,[1, a)] P. Dmitruk,[1] P.D. Mininni,[1] and W.H. Matthaeus[2]
[1)] *Departamento de Física, Facultad de Ciencias Exactas y Naturales, Universidad de Buenos Aires and IFIBA, CONICET, Ciudad universitaria, 1428 Buenos Aires, Argentina*
[2)] *Bartol Research Institute and Department of Physics and Astronomy, University of Delaware, Newark, Delaware, USA*

The effect of compressibility in charged particle energization by magnetohydrodynamic (MHD) fields is studied in the context of test particle simulations. This problem is relevant to the solar wind and the solar corona due to the compressible nature of the flow in those astrophysical scenarios. We consider turbulent electromagnetic fields obtained from direct numerical simulations of the MHD equations with a strong background magnetic field. In order to explore the flow compressibilty effect over the particle dynamics we performed different numerical experiments: an incompressible case, and two weak compressible cases with Mach number $M = 0.1$ and $M = 0.25$. We analyze the behavior of protons and electrons in those turbulent fields, which are well known to form aligned current sheets in the direction of the guide magnetic field. What we call protons and electrons are test particles with scales comparable to (for protons) and much smaller than (for electrons) the dissipative scale of MHD turbulence, maintaining the correct mass ratio m_e/m_i. For these test particles we show that compressibility enhances the efficiency of proton acceleration, and that the energization is caused by perpendicular electric fields generated between currents sheets. On the other hand, electrons remain magnetized and display an almost adiabatic motion, with no effect of compressibility observed. Another set of numerical experiments takes into account two fluid modifications, namely electric field due to Hall effect and electron pressure gradient. We show that the electron pressure has an important contribution to electron acceleration allowing highly parallel energization. In contrast, no significant effect of these additional terms is observed for the protons.

I. INTRODUCTION:

Turbulence is an ubiquitous phenomenon in many astrophysical environments, in which a wide variety of temporal and spatial scales are involved. This is the case of the solar wind or the intellestar medium where the energy is transferred from large to small kinetic scales where the energy is dissipated. In the macroscopic description of a plasma, magnetohydrodynamics (MHD) turbulence is the result of the nonlinear interaction of fluctuations of the velocity and magnetic fields, leading to a spatial intermittency that is associated with coherent structures, and where the dissipation is concentrated in strong gradient regions that impact on the heating, transport and particle acceleration in plasmas[1].

The efficiency of MHD turbulence to accelerate charged particles and its importance in space physics has been reported by many different authors[2–4], but the great variety of scales involved in turbulence and the particle dynamics makes this a challenging problem. On long timescales (large eddy turnover times) dynamics is governed by stochastic acceleration, and momentum diffusion is the main acceleration mechanism which has been mainly applied for cosmic-ray energization studies and frequently addressed by quasi-linear theory (QLT)[5–7]. In diffusion studies MHD turbulence is commonly represented as a random collection of waves, and that representation lacks coherent structures that have an important role at particle scales[8]

Dmitruk et al 2004[9], using test particle simulations in static electromagnetic fields obtained from direct numerical simulation (DNS) of the MHD equations, showed that particle energization at dissipation scales is due to current sheets, and the acceleration mechanism depends on the particle gyroradii. By static electromagnetic fields, here we mean that the fields are dynamically computed in a turbulent and self-consistent MHD simulation, and then a snapshot is extracted and the fields are frozen to compute particle trajectories and acceleration.

Using a more sophisticated model, but still using static turbulent electromagnetic fields, Dalena et al 2012[10] showed essentially the same results. Electrons initially moving with Alfvén velocity experience parallel (to the guide magnetic field) acceleration by parallel electric fields inside current sheet chanels. On the other hand, protons are accelerated in a two stage process: Initially they are parallelly accelerated and gain substantial energy in a short time. Then, when the proton gyroradius becomes comparable to the current sheet thickness, protons are accelerated perpendicular to the guide field.

[a)] Electronic mail: caangonzalez@df.uba.ar

Effects of compressible MHD on particle energization has been reported in diffusion studies[11,12], where supersonic turbulence was considered. There are also reports of test particle pitch angle scattering in compressible MHD turbulence[13] considering second order Fermi acceleration by weak compressible MHD running simultaneously the test particles and MHD fields, and imposing a scattering rate. It was found that compressibility is important to produce non-thermal particles. Additionally, there are other studies where test particles and fields are simultaneously advanced in time. Weidl et al 2015[14] and Teaca et al. 2014[15] used an incompressible MHD model, analyzing the effect of the correlation between magnetic and velocity fields on pitch-angle scattering and particle acceleration. They found that imbalanced turbulence (nonzero cross-helicity in the system) reduces the particle acceleration and also the pitch angle scattering.

In the present work we are interested in the compressibility effect on particle acceleration by coherent structures in static electromagnetic fields stemming from a direct numerical simulation of the MHD equations, and in the identification of the fields which accelerate the particles. We analyze the particle behavior for three different situations: an incompressible case, and two weakly compressible cases with differing values of the sonic Mach number. We also consider the effect of the Hall current and of electron pressure in the acceleration. The organization of this paper is as follows: In section 2 we describe the model employed in our investigation, the equations and properties of turbulent MHD fields, and the test particle model including the parameters that correlate particles and fields. In sections 3 and 4 we show the properties of proton and electron dynamics. Finally, in section 5 we discuss our findings and present our conclusions.

II. MODELS:

The macroscopic description of a plasma adopted here is the system of the three-dimensional compressible MHD equations: the continuity (density) equation, the equation of motion, the magnetic field induction equation, and the equation of state. These are Eqs. (1-4) respectively, which involve fluctuations of the velocity field $\mathbf{u}$, magnetic field $\mathbf{b}$, and density ρ. We assume a large-scale background magnetic field B_0 in the z-direction, so that the total magnetic field is $\mathbf{B} = \mathbf{B_0} + \mathbf{b}$

$$\frac{\partial \rho}{\partial t} + \nabla \cdot (\mathbf{u}\rho) = 0, \tag{1}$$

$$\frac{\partial \mathbf{u}}{\partial t} + \mathbf{u}\cdot\nabla\mathbf{u} = -\frac{\nabla p}{\rho} + \frac{\mathbf{J}\times\mathbf{B}}{4\pi\rho} + \nu\left(\nabla^2\mathbf{u} + \frac{\nabla\nabla\cdot\mathbf{u}}{3}\right), \tag{2}$$

$$\frac{\partial \mathbf{B}}{\partial t} = \nabla \times (\mathbf{u}\times\mathbf{B}) + \eta\nabla^2\mathbf{B}, \tag{3}$$

$$\frac{p}{\rho^\gamma} = \text{constant}. \tag{4}$$

Here p is the pressure, ν the viscosity, η the magnetic diffusivity, and $\mathbf{J} = \nabla \times \mathbf{B}$ is the current density. We assume a polytropic equation of state $p/p_0 = (\rho/\rho_0)^\gamma$, with $\gamma = 5/3$, where p_0 and ρ_0 are respectively the equilibrium (reference) pressure and density. We consider two weak compressible cases with Mach number ($M = \sqrt{\gamma p_0/\rho_0}$) equal to $M = 0.1$ and $M = 0,25$. Additionally, in order to have a reference to measure the effect of compressibility on particle acceleration, we consider an incompressible case (with $\nabla \cdot \mathbf{u} = 0$ and $\rho =$ a uniform constant).

The magnetic and velocity fields are here expressed in Alfvén speed units; a characteristic plasma velocity is given by the parallel Alfvén wave velocity along the mean magnetic field $v_A = B_0/\sqrt{4\pi\rho_0}$. An Alfven speed based on field fluctuations can also be defined as $v_0 = \sqrt{\langle b^2\rangle/4\pi\rho_0}$. The ratio of the fluctuating to the mean magnetic field is $\langle b\rangle/B_0 \approx 0.1$. The ratio of fluid equilibrium pressure p_0 to magnetic pressure B_0^2, the so-called β of the plasma, is $\beta = p_0/B_0^2 = 1/(M^2B_0^2) = 0.25$. We take v_0 as a unit for velocity and magnetic field fluctuations. We use the isotropic MHD turbulence correlation length L as a characteristic length (also called the energy containing scale), defined as $L = 2\pi\int(E(k)/k)dk/\int E(k)dk$ where $E(k)$ is the energy at wavenumber k. The value of this scale for our simulations is $L = 1.3$, as compared to the box size $L_{box} = 2\pi$. The unit timescale t_0, also called eddy turnover time, is derived from the unit length and the fluctuation Alfven speed $t_0 = L/v_0$. We note that our simulations do not have exact equipartition between magnetic and kinetic energy, this ratio being $E_m/E_k \approx 0.8$. The initial magnetic and velocity field fluctuations populate an annulus in Fourier k-space defined by a range of wavenumbers with $3 \le k \le 4$, with constant amplitudes and random phases.

The MHD equations are solved numerically using a Fourier pseudospectral method with periodic boundary conditions in a cube of size L_{box}; this scheme ensures exact energy conservation for the continuous time spatially discrete equations[16]. The discrete time integration is done with a high-order Runge-Kutta method, and a resolution of (256^3) Fourier modes is used. For the kinematic Reynolds number $R = v_0L/\nu$ and the magnetic Reynolds number $R_m = v_0L/\eta$, we take $R = R_m = 1000$, which are limited here by the available spatial resolution.

When the turbulence is fully-developed a broad range of scales develops, from the outer scale L to the Kolmogorov dissipation scale $l_d = (\nu^3/\epsilon_d)^{1/4}$, with ϵ_d the average rate of energy dissipation. For the simulations it is $l_d \approx 1/32$. We then employ a snapshot of this turbulent MHD state in which to evolve the test particles. The behavior of a test particle in an electromagnetic field is described by the nonrelativistic particle equation of motion:

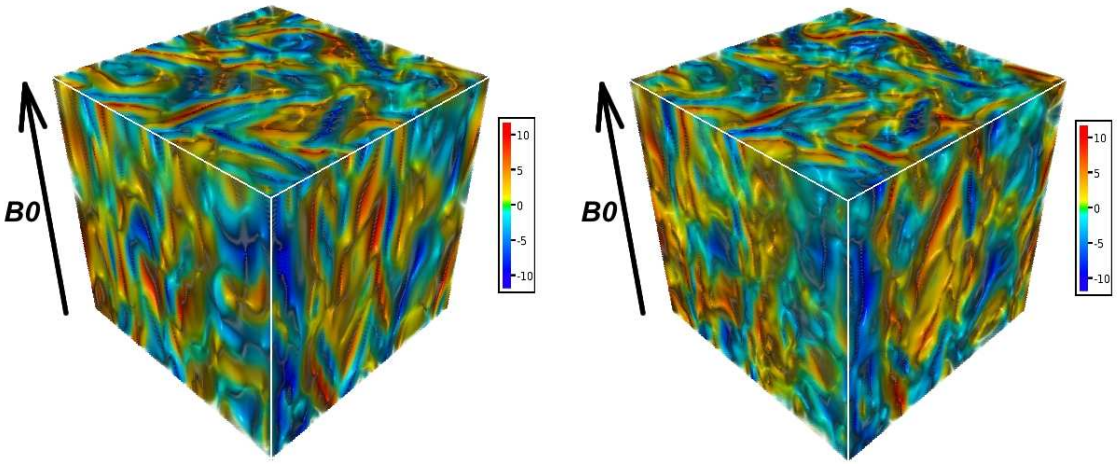

FIG. 1. Three-dimensional view of the parallel current density $J_z(x, y, z)$. (Left) Incompressible and (Right) Compressible case with Mach number $M = 0.25$ at $t/t_0 = 2$.

$$\frac{d\mathbf{v}}{dt} = \alpha(\mathbf{E} + \mathbf{v} \times \mathbf{B}), \qquad \frac{d\mathbf{r}}{dt} = \mathbf{v}. \tag{5}$$

The nondimensional electric field $\mathbf{E}$ is obtained from Ohm's law normalized with $E_0 = v_0 B_0/c$ as follows:

$$\mathbf{E} = -\mathbf{u} \times \mathbf{B} + \frac{\mathbf{J}}{R_m}. \tag{6}$$

Finally the adimensional parameter α relates particles and MHD field parameters:

$$\alpha = Z\frac{m_p}{m}\frac{L}{\rho_{ii}}, \tag{7}$$

where ρ_{ii} is the proton inertial length given by $\rho_{ii} = m_p c/(e\sqrt{4\pi\rho_0})$, m is the mass of the particle, m_p is the mass of the proton, and Z is the atomic number ($Z = 1$ for protons and electrons). The inverse $1/\alpha$ represents the nominal gyroradius, in units of L and with velocity v_0 and measures the range of scales involved in the system (from the outer scale of turbulence to the particle gyroradius). One could expect a value $\alpha \gg 1$ specially for space physics and astrophysical plasmas. This represent a huge computational challenge due to numerical limitations. As stated above, we consider here a dissipation length scale $l_d \approx 1/32$, which is also of the order of the current sheet thickness.

In the fixed MHD turbulence state, 10000 test particles are randomly distributed in the computational box and the equation of motion of particles subject to the MHD electromagnetic field are solved using a second-order Runge-Kutta method. Furthermore, we use high order spline interpolation to compute the field values on each particle position.

Particles are initialized with a Gaussian velocity distribution function with a root mean square (rms) value of the order of the Alfven velocity. It is well known that the particle gyroradius has a significant influence on acceleration, and our aim in this paper is to explore the compressibility effect on acceleration of large gyroradius and small gyroradius particles. In the next section we show two different compressible cases with Mach number $M = 0.25$ and $M = 0.1$, as well as an incompressible case. In all cases the mean magnetic field is set to $B_0 = 10$. We present the behavior of protons with a nominal (speed v_0) gyroradius 1/32, and electrons ($m_e = m_p/1836$) with nominal gyroradius 1/58752.

III. FLOW COMPRESSIBILITY EFFECTS (FCE):

In Figure 1 a three-dimensional view of the z-component of the current density $J_z(x, y, z)$ is shown at $t = 2.5t_0$ for the incompressible case and a compressible case with $M = 0.25$. It is observed that current sheets are aligned in the direction of the guide magnetic field. It can also be seen that in both cases the structures are similar, but more corrugated in the compressible case and smoother in the incompressible one. It is worth mentioning that we used the same initial conditions for all the simulations. Coherent structures like these show the natural tendency of the MHD equations to develop strong gradients leading to many reconection zones, which is well known to be one of the mechanisms behind charged particle acceleration. Figure 2 shows the spectrum of kinetic (top) and magnetic energy (bottom) for the compressible cases with $M = 0.25$ and $M = 0.1$, and the incompressible case. In the inertial range there are almost no differences between the compressible and incompressible energy spectra for both magnetic and velocity fields, although slightly more energy at large scales is observed in the incompressible case. On the other hand, at wavenumbers beyond the dissipation scale (that is, for

$k \geq 32$), an excess of energy is observed as the Mach number is increased. This feature is more evident for the kinetic energy spectrum than for the magnetic energy spectrum. Since protons mostly interact with structures of that size, this can be an important effect on proton acceleration. In order to explore the importance of compressible effects on MHD fields, we make a Helmholtz decomposition of the velocity field, presented in the inset in Fig 2, where $\hat{\mathbf{v}}_\mathbf{T}(\mathbf{k}) = (\mathbf{I} - \hat{\mathbf{k}}\hat{\mathbf{k}})\mathbf{u}(\mathbf{k})$ represents the solenoidal (incompressible) part and $\hat{\mathbf{v}}_\mathbf{L}(\mathbf{k}) = \hat{\mathbf{u}}(\mathbf{k}) - \hat{\mathbf{v}}_\mathbf{T}(\mathbf{k})$ is the irrotational (compressive) component. It is observed that at high k the velocity field spectrum is strongly compressible, and that compression becomes more prominent at higher turbulent Mach number. The large k effects in the compressible kinetic spectrum may be attributed to the emergence of shock-like structures that enhance the energy in the smallest scales, as compared to the incompressible case.

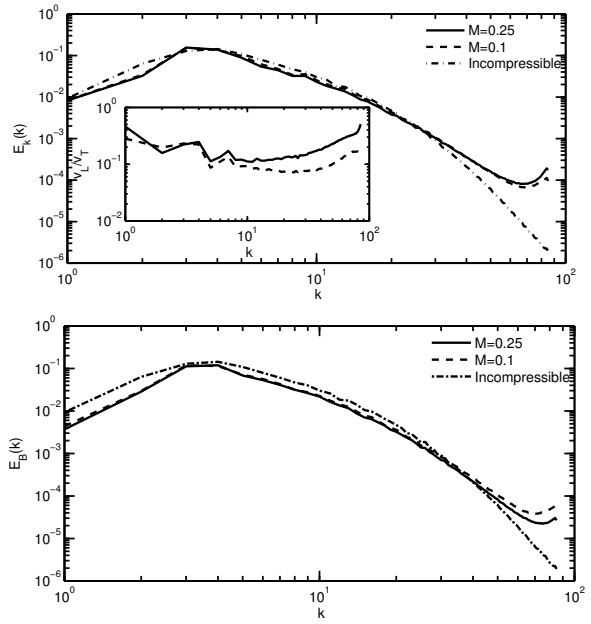

FIG. 2. (Top) Kinetic energy spectrum for compressible cases with Mach numbers $M = 0.25$ (solid line), $M = 0.1$ (dashed line), and incompressible case (dashed-dot line); the inset shows the ratio between solenoidal and irrotational (compressive) components of the velocity field for compressible runs. (Bottom) Magnetic energy spectrum for the three cases mentioned before, using the same labels.

Protons. We remark here that what we call "protons" are test particles with gyroradius comparable to the dissipative scale of the MHD turbulence, although the MHD approximation is only marginally valid at those small scales. Figure 3 shows the time evolution for the mean value of the perpendicular $v_\perp = \sqrt{v_x^2 + v_y^2}$ (top) and parallel $v_\parallel = v_z$ (bottom) proton velocity, relative to B_0, for the compressible ($M = 0.25$, $M = 0.1$) cases and the incompressible case. The typical acceleration process observed in previous studies is evident, proton are accelerated perpendicularly with respect to B_0, while they are less accelerated parallely.

Moreover, the compressibility effect on particle acceleration is clearly observed. Protons are highly accelerated as compressibility of the fluid increases, for both perpendicular and parallel directions. Acceleration of protons is also observed in the incompressible case (see inset plot) but the value of the velocity reached at the end of the simulation is much lower than in both compressible cases, even with relatively small values of the Mach number M as the ones considered here.

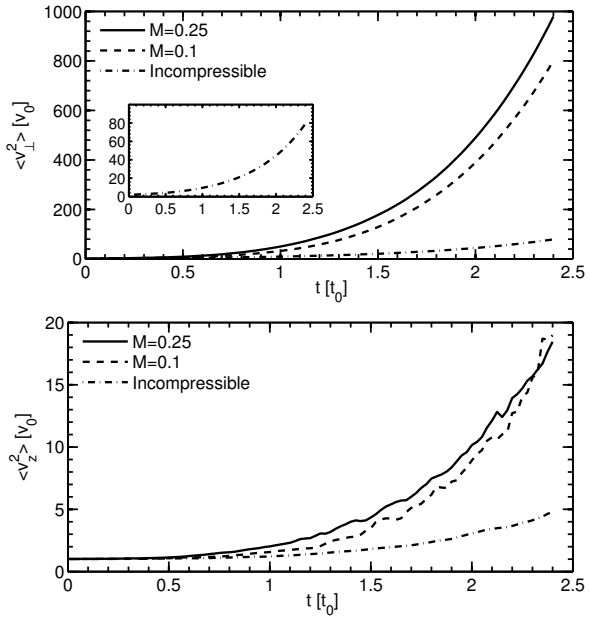

FIG. 3. Particle mean square velocity as a function of time: (Top) Proton perpendicular velocity $v_\perp = \sqrt{v_x^2 + v_y^2}$ for two different Mach number cases, $M = 0.25$ (solid line), $M = 0.1$ (dashed line), and the incompressible case (dash-dot line); the inset shows a detail of the proton perpendicular mean square velocity for the incompressible case.

(Bottom) Proton parallel velocity $v_\parallel = v_z$ for $M = 0.25$, $M = 0.1$, and incompressible case, with the same labels for the lines.

Figure 4 shows the probability distribution function (PDF) of the perpendicular x-component (top) and of the parallel z-component (bottom) of the electric field for the compressible and incompressible cases. The PDF shows that, as compression increases, long tails in the distribution arise and higher values of the perpendicular electric field are achieved. Additionally, the core part of the distribution function for the incompressible case is thicker than for the compressible cases. On the other hand, the PDF of the parallel electric field shows very little effect of increasing compressibility. In order to better understand the dynamics of protons, in Figure 5 we show the current density $J_z(x, y, z)$ together with the trajectory of one of the most energetic protons,

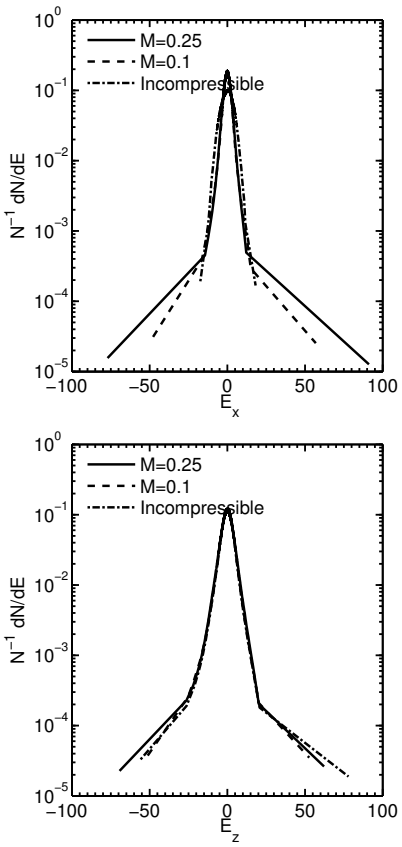

FIG. 4. Probability density function of electric field components in the simulation. (Top) Perpendicular x-component for $M = 0.25$ (solid line), $M = 0.1$ (dashed line), and incompressible (dash-dot line). (Bottom) Parallel z-component of the electric field using the same labels.

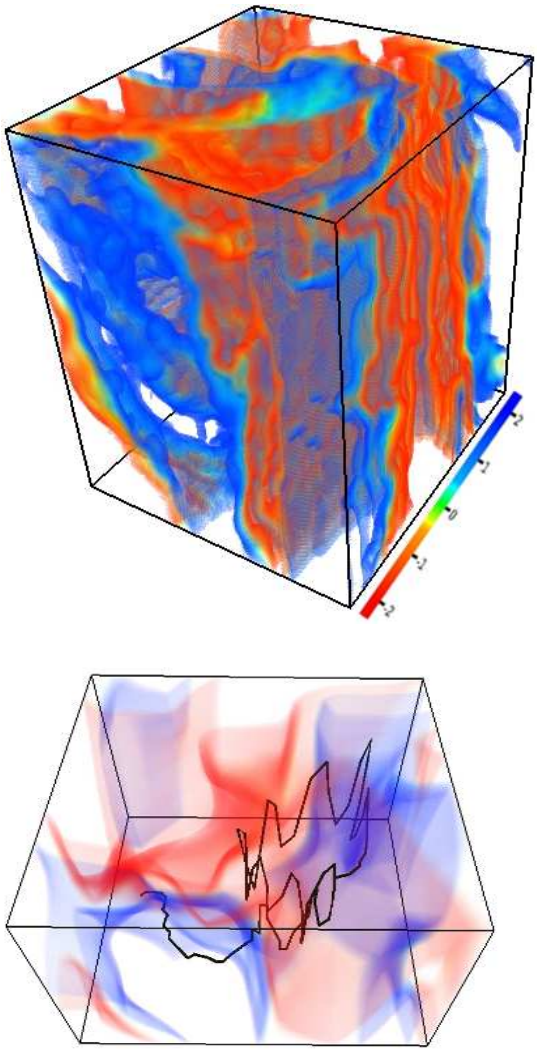

FIG. 5. (Top) View of the parallel current density $J_z(x, y, z)$. (Bottom) Trajectory of one of the most energetic protons; the z-component of the current density is shown in the transparent volume rendering.

for the compressible $M = 0.25$ case. The visualization was done using the software VAPOR[17]. It is observed that on the surrounding of the particle trajectory there are many current sheets, which contribute to the proton energization. Figure 6 shows the values of quantities following the trajectory of the most energetic proton, that is, the most energetic proton is identified and the values of several quantities along the trajectory of this proton are obtained: (a) the current density J_z, (b) electric field components E_x, E_y, E_z, (c) proton velocity components v_x, v_y, v_z and (d) root mean square displacement of the proton. The panels on the left correspond to the compressible $M = 0.25$ case, and the panels on the right correspond to the incompressible case.

It is observed that when there is a change of the sign in the current density J_z, there is also an increment in the perpendicular components of the electric field that the particle experiences, and concurrently there is an increment of the proton velocity. This situation is repeatedly observed in time as the energy of the proton increases.

A possible explanation for the change of sign in the current density is that the particle is entering and leaving two neighboring current sheets with different polarities while experiencing a strong perpendicular electric field between those current sheets. The perpendicular electric field is stronger as the compression of the fluid increases (this can be noticed by comparing panels on the left and right of Figure 6). Consequently, the velocity increment is larger in the compressible case than in the incompressible case. This situation can be generalized for many particles in the simulation, resulting in the increase of the root mean square velocity for the ensemble of particles.

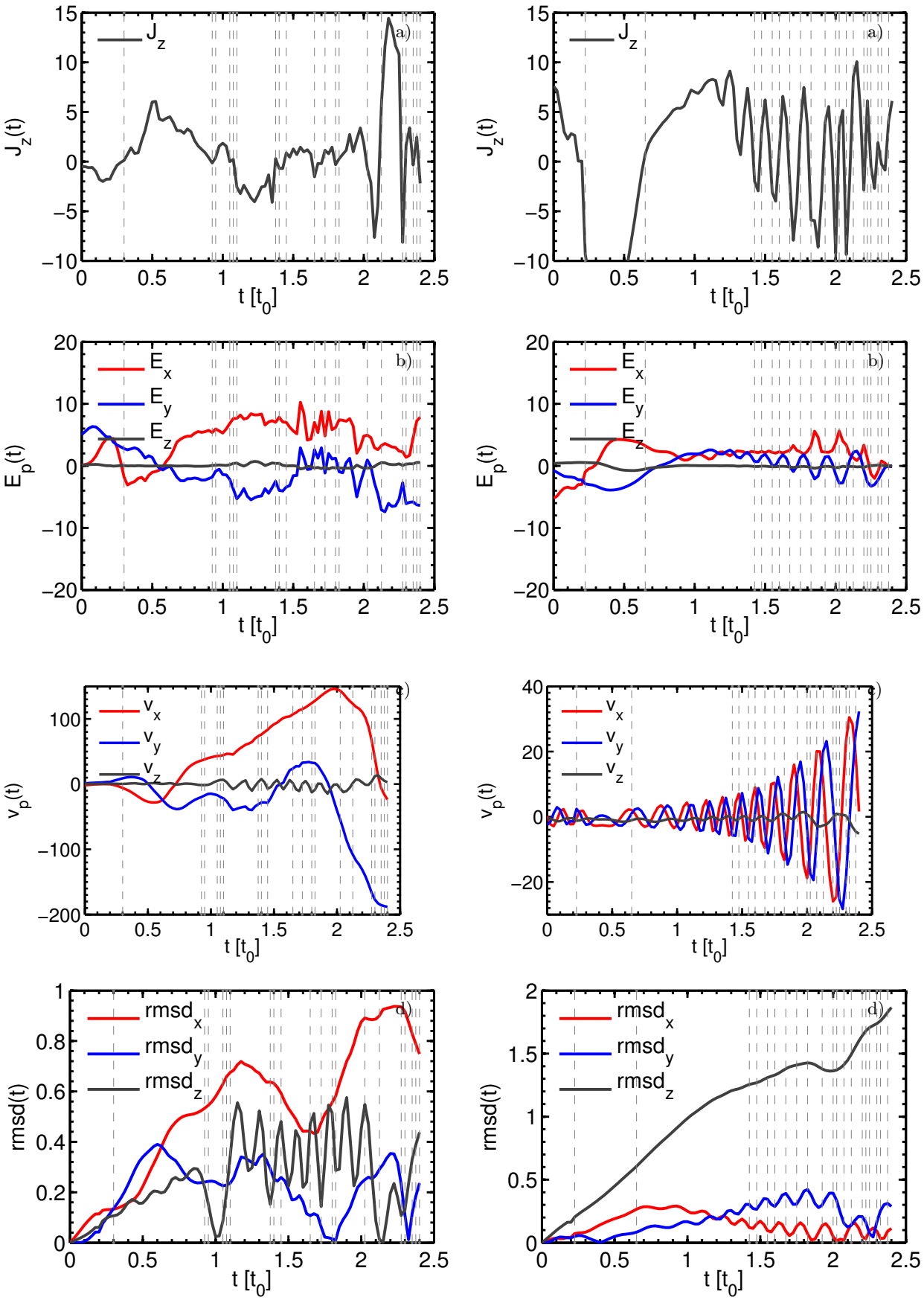

FIG. 6. (a) Parallel current density, (b) the three components of the electric field, (c) velocity components, and (d) rms displacement as function of time for the most energetic particle: (Left) compressible $M = 0.25$ case and (Right) incompressible case. The gray vertical dashed-lines show the moments when current is reversed.

The reason for greater perpendicular electric field in the compressible cases can be understood in terms of the magnetic flux pileup that accompanies the interaction of adjacent flux tubes in turbulence[18]. While current sheets typically form between interacting flux tubes, when the flux tubes are driven together by the turbulent flow, there is also frequently a magnetic flux pileup near the boundary. This compression of the magnetic field occurs in the incompressible case as well, but clearly can be greater when the material elements themselves are compressible. The pileup phenomenon is readily seen to be associated with reversal of the electric current density. Furthermore, the parallel magnetic flux increases due to this compression, requiring a circulation of the perpendicular electric field vector, thus setting the scene for betatron acceleration[10].

Electrons. What we call "electrons" are test particles with gyroradius much smaller than the dissipative scale of MHD turbulence. At those scales MHD is not expected to be valid anymore. However, we maintain the correct ratio of electron to proton mass, $m_e/m_p = 1/1836$. In the next section we discuss other relevant effects at those scales.

Figure 7 shows the time evolution for the perpendicular (top) and z-component (bottom) of electron rms velocity for the compressible ($M = 0.25$, $M = 0.1$) and incompressible cases. It should be mentioned that we are showing a short time simulation of electrons here. This is due to the high computational cost of integrating the trajectory of electrons in a flow, as electrons require a very small time step (to represent a physical small gyroradius). The total time reached in the electron simulations is of the order of almost 3000 electron gyroperiods. Electrons present the typical parallel energization reported in previous works. Besides, there is no evidence that compression of the MHD fields substantially enhances the electron acceleration, as electrons gain almost the same energy regardless the compressible level of the fluid. Since the gyradius of electrons is smaller than any of the length scales of structures in the fields, when electrons find a current sheet they travel along magnetic field lines and there is not so much difference between compressible and incompressible cases.

Also, the perpendicular rms velocity shows that electrons are initially accelerated but quickly exhibit a constant perpendicular energy. Constant perpendicular energy is consistent with near conservation of the magnetic moment, which is one of the adiabatic invariants of charged particle dynamics in a magnetic field.

It is important to remark that over longer timescales, of the order of many turnover times, electrons can obtain very high parallel energy, and it is likely that the motion will no longer be adiabatic. In that case, electrons can reach other regions and interact with structures that generate other possible acceleration mechanisms, such as those that involve pitch angle-scattering, betatron acceleration, etc.

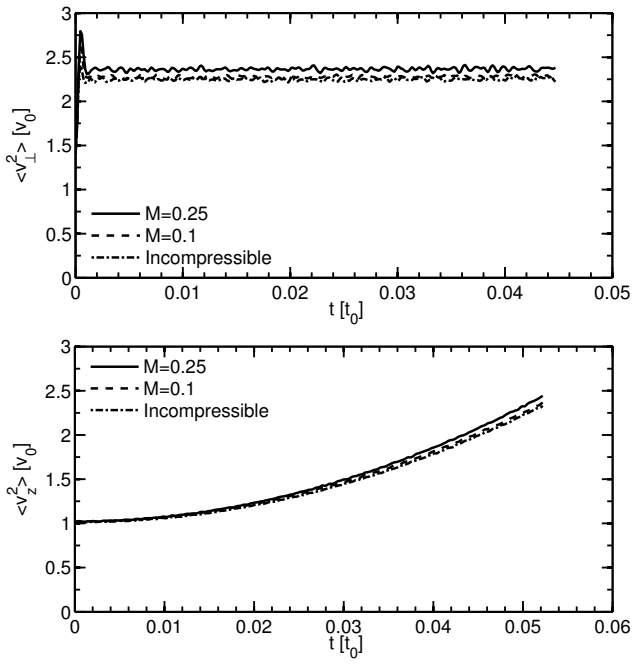

FIG. 7. (Top) Time evolution of the perpendicular rms velocity for electrons, for the compressible cases with $M = 0.25$ (solid line), $M = 0.1$ (dashed line), and the incompressible case (dot-dashed line). (Bottom) Time evolution of the parallel rms velocity for electrons, using the same notation.

IV. ELECTRON PRESSURE EFFECTS (EPE):

In this section we consider additional effects in the electric field which were not taken into account in the previous section. As will be seen, these effects are important for the electrons but not so for the protons. Adopting a generalized Ohm's law from a two-fluid plasma description, the electric field becomes

$$\mathbf{E} = -\mathbf{u} \times \mathbf{B} + \frac{\epsilon}{\rho}\mathbf{J} \times \mathbf{B} - \epsilon \nabla p_e + \frac{\mathbf{J}}{R_m}. \qquad (8)$$

written in a dimensionless form.

The additional terms as compared to Eq. (6) are the Hall effect term $\mathbf{J} \times \mathbf{B}/\rho$ and the electron pressure gradient term ∇p_e. The dimensionless coefficient ϵ multiplying terms is the Hall parameter:

$$\epsilon = \frac{\rho_{ii}}{L} \qquad (9)$$

which relates the ion inertial length scale with the energy containing scale. For consistency with the test particles definition (see Eq. (7)) we set the value of the Hall parameter $\epsilon = 1/\alpha = 1/32$ in our simulations, where $1/\alpha$ is the nominal gyroradius of the protons. In the MHD description it is assumed that plasma protons and electrons are in thermal equilibrium, i.e, their pressures are $p_e = p_i$. Then $p_e = p/2$ with $p = p_e + p_i$ the total pressure. It is worth mentioning that Dmitruk et al 2006[19]

previously analyzed the Hall effect only, not considering electron pressure effects, and did not see a significant contribution of this effect in the particles acceleration.

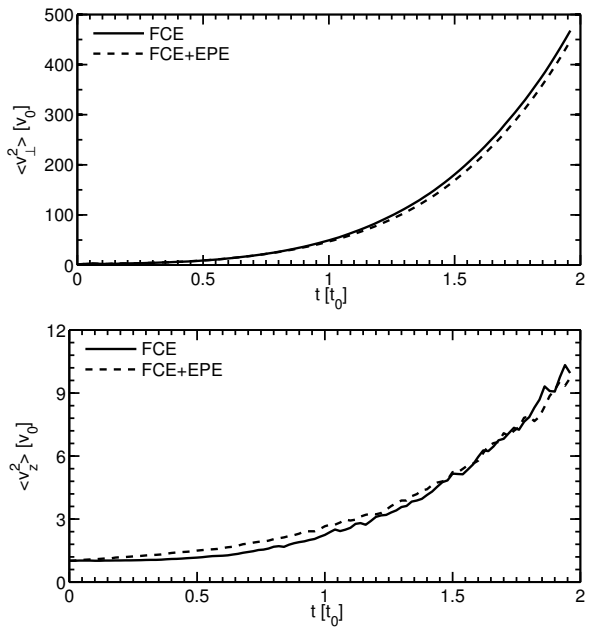

FIG. 8. Proton mean square velocity as a function of time considering flow compressibility effects (FCE), and considering flow compressibility plus electron pressure effects (FCE+EPE): (Top) Proton perpendicular velocity $v_\perp = \sqrt{v_x^2 + v_y^2}$ with FCE (solid line) and with FCE+EPE (dashed line), both for the case with $M = 0.25$. (Bottom) Proton parallel velocity $v_\parallel = v_z$, with the same labels for all curves.

In order to measure the effect of electron pressure on test particle energization we compared the proton and electron energization for the case with $M = 0.25$, taking into account the flow compressibility effect (FCE) only, and the flow compressibility effect plus the electron pressure effect (FCE+EPE). The results are shown in Figures 8 and 9.

Figure 8 shows the perpendicular (top) and parallel rms velocity (bottom) for protons. It is observed that no significant contribution of EPE occurs for proton energization, and the main particle acceleration mechanism remains the interaction with current sheets as discussed in the previous section.

In contrast a very different situation is observed for electrons, as shown in Figure 9. The electron behavior is no longer magnetized and the non constant perpendicular energy (top panel) represents non-adiabatic motion. As seen in Fig. 9 (bottom panel) a very high parallel energy (that is, high square parallel velocity) is reached in a short time, showing the importance of the EPE for electrons in compressible MHD.

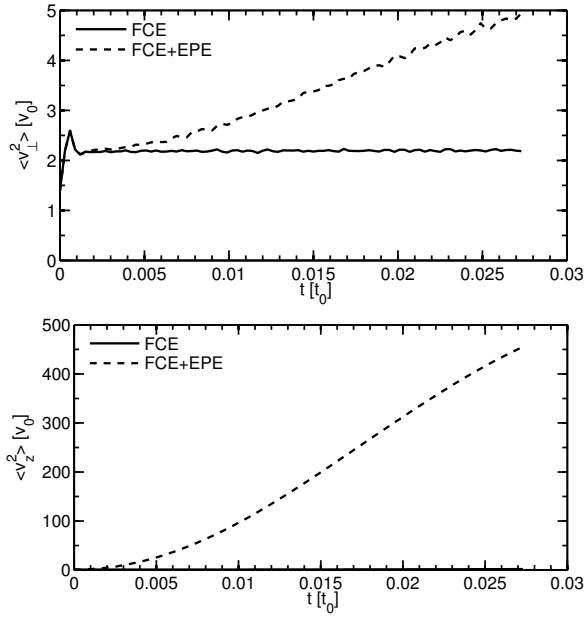

FIG. 9. Electron mean square velocity as a function of time considering flow compressibility effects (FCE), and considering flow compressibility effects plus electron pressure effects (FCE+EPE): (Top) Electron perpendicular velocity $v_\perp = \sqrt{v_x^2 + v_y^2}$ for FCE (solid line) and FCE+EPE (dashed line) for the case $M = 0.25$. (Bottom) Mean square parallel (v_z^2) electron velocity. Note that increase in FCE only case is small as in Fig 7

V. DISCUSSION:

We investigated the effect of compressible MHD turbulence on particle energization, using test particle simulations in frozen electromagnetic fields obtained from direct numerical solutions of the MHD equations. We found that flow compressibility affects the energization of protons (i.e., in the context of this work, test particles with gyroradius of the order of the MHD dissipation scale), while no significant effect is observed for electrons (particles with gyroradius much smaller than the MHD dissipation scale) as compared with the incompressible case.

Protons are accelerated by the perpendicular electric field generated on the interface of current sheets, and they gain substantial energy as they encounter these structures. Moreover, the perpendicular electric field between current sheets is greater as compression of the fluid increases, leading to a higher proton acceleration.

On the other hand, small gyroradii particles remain magnetized and gain parallel energy as they travel along magnetic field lines almost aligned with B_0. No effect of compressibility is noted for these kind of particles and this is because the compressible modes in magnetohydrodynamics are perpendicular propagating modes ($k \perp B_0$). As a result no difference in the parallel electric field obtained from static MHD fields is presented.

An interesting result is that when the model includes electron pressure gradients effects in the electric field, obtained from the generalized Ohm's law, one finds substantially greater parallel energization of electrons. In contrast, no significant changes are obtained for the proton energization with the inclusion of the electron pressure gradient effects and of Hall currents.

The main aim of this paper was to analyze the case of weakly compressible turbulence, often appropriate to study the solar wind and other astrophysical scenarios, even though these plasmas can sometimes attain a strongly compressible state ($M \geq 1$). We can thus conclude that at least for low turbulent Mach number, compression can enhance particle energization associated with coherent structures and therefore it has important implications for the study of particle acceleration by turbulent fields. In the incompressible case, which is the limit of infinite sound wave velocity, protons can still be accelerated, but less than in the compressible case. The incompressible case thus served as a reference to measure the influence of compression on particle acceleration. Also, the incompressible case can still be relevant for some real physical scenarios, such as the fast solar wind which might energize particles as well[15].

We close with a remark concerning the importance of trapping effects in acceleration of particles to higher energies in compressible turbulence. In general, for effective energization the particles must be exposed to a suitable electric field, but also the trajectory of the particle must allow a long exposure time of the particle to the accelerating field. In the present case, parallel acceleration of electrons occurs when their gyroradii are small compared to the width of mean field-aligned current channels, as noted previously by Dmitruk et al. [9]. Analogous trapping effects due to confinement in magnetic "islands" has been noted in various systems from two dimensional MHD[20] to fully kinetic PIC simulations[21]. In those scenarios small gyroradius particle are trapped for a period of time sufficient for them to experience substantial parallel energization. Depending on parameters this may be either heating (more particles, lower energies) or acceleration (less particles but higher energy). On the other hand, protons, having larger gyroradius, will not be easily trapped in current channels, which often are a few proton inertial scales in width.

The perpendicular acceleration mechanism described previously[9,10] and elaborated on here, provides a way to accelerate protons (and heavier ions) due to pependicular electric fields. The region of interaction between flux tubes provides the possibility of generating regions of effective acceleration that may lie between reversing currents. Although these may be very complex regions in three dimensions, in a simplified two dimensional picture these can be flux pileup regions with gradients of the perpendicular electric field. This transverse compression of the magnetic field may occur even when the turbulence is incompressible. It is, however intuitively clear that compressibility will permit greater pileup and greater perpendicular electric field gradients. In addition, to produce an efficient accelerator, the particles must also be trapped in the accelerating region for sufficient time. The present numerical experiments also suggest that compressibility of the turbulence, acting near and within the regions between reversing currents, may provide substantially enhanced trapping for some particles. This is needed to explain the significantly greater perpendicular acceleration observed here when the turbulence is compressible.

ACKNOWLDEGMENTS

The authors thank an anonymous reviewer for useful comments that resulted in the study of electron pressure effects. C.A.G, P.D., and P.D.M. acknowledge support from grants UBACyT No. 20020110200359 and 20020100100315, and from grants PICT No. 2011-1529, 2011-1626, and 2011-0454. W.H.M. was partially supported by NASA LWS-TRT grant NNX15AB88G, Grand Challenge Research grant NNX14AI63G, and the Solar Probe Plus mission through the Southwest Research Institute ISIS project D99031L.

[1] W. H. Matthaeus, Minping Wan, S. Servidio, A. Greco, K. T. Osman, S. Oughton, and P. Dmitruk. *Philosophical Transactions of the Royal Society of London A: Mathematical, Physical and Engineering Sciences*, 373(2041), 2015. ISSN 1364-503X. doi: 10.1098/rsta.2014.0154.

[2] ENRICO Fermi. *Phys. Rev.*, 75:1169–1174, Apr 1949. doi: 10.1103/PhysRev.75.1169. URL `http://link.aps.org/doi/10.1103/PhysRev.75.1169`.

[3] A. Lazarian, L. Vlahos, G. Kowal, H. Yan, A. Beresnyak, and E.M. de GouveiaDalPino. *Space Science Reviews*, 173(1-4):557–622, 2012. ISSN 0038-6308. doi:10.1007/s11214-012-9936-7. URL `http://dx.doi.org/10.1007/s11214-012-9936-7`.

[4] W. H. Matthaeus, J. J. Ambrosiano, and M. L. Goldstein. *Phys. Rev. Lett.*, 53:1449–1452, Oct 1984. doi: 10.1103/PhysRevLett.53.1449. URL `http://link.aps.org/doi/10.1103/PhysRevLett.53.1449`.

[5] Reinhard Schlickeiser and James A. Miller. *The Astrophysical Journal*, 492(1):352, 1998. URL `http://stacks.iop.org/0004-637X/492/i=1/a=352`.

[6] Benjamin D. G. Chandran and Jason L. Maron. *The Astrophysical Journal*, 603(1):23, 2004. URL `http://stacks.iop.org/0004-637X/603/i=1/a=23`.

[7] Lange, S., Spanier, F., Battarbee, M., Vainio, R., and Laitinen, T. *A&A*, 553:A129, 2013. doi:10.1051/0004-6361/201220804. URL `http://dx.doi.org/10.1051/0004-6361/201220804`.

[8] Kaspar Arzner and Loukas Vlahos. Particle acceleration in multiple dissipation regions. *The Astrophysical Journal Letters*, 605 (1):L69, 2004. URL `http://stacks.iop.org/1538-4357/605/i=1/a=L69`.

[9] Pablo Dmitruk, W. H. Matthaeus, and N. Seenu. *The Astrophysical Journal*, 617(1):667, 2004. URL `http://stacks.iop.org/0004-637X/617/i=1/a=667`.

[10] S. Dalena, A. F. Rappazzo, P. Dmitruk, A. Greco, and W. H. Matthaeus. *The Astrophysical Journal*, 783(2):143, 2014. URL `http://stacks.iop.org/0004-637X/783/i=2/a=143`.

[11] Benjamin D. G. Chandran. *The Astrophysical Journal*, 599(2): 1426, 2003. URL `http://stacks.iop.org/0004-637X/599/i=2/a=1426`.

[12] Jungyeon Cho and A. Lazarian. *The Astrophysical Journal*, 638 (2):811, 2006. URL http://stacks.iop.org/0004-637X/638/i=2/a=811.

[13] Jacob W. Lynn, Eliot Quataert, Benjamin D. G. Chandran, and Ian J. Parrish. *The Astrophysical Journal*, 777(2):128, 2013. URL http://stacks.iop.org/0004-637X/777/i=2/a=128.

[14] Martin S. Weidl, Frank Jenko, Bogdan Teaca, and Reinhard Schlickeiser. *The Astrophysical Journal*, 811(1):8, 2015. URL http://stacks.iop.org/0004-637X/811/i=1/a=8.

[15] Bogdan Teaca, Martin S. Weidl, Frank Jenko, and Reinhard Schlickeiser. *Phys. Rev. E*, 90:021101, Aug 2014. doi: 10.1103/PhysRevE.90.021101. URL http://link.aps.org/doi/10.1103/PhysRevE.90.021101.

[16] Pablo D. Mininni, Duane Rosenberg, Raghu Reddy, and Annick Pouquet. A hybrid mpiopenmp scheme for scalable parallel pseudospectral computations for fluid turbulence. *Parallel Computing*, 37(67):316 – 326, 2011. ISSN 0167-8191. doi:http://dx.doi.org/10.1016/j.parco.2011.05.004. URL http://www.sciencedirect.com/science/article/pii/S0167819111000512.

[17] John Clyne, Pablo Mininni, Alan Norton, and Mark Rast. Interactive desktop analysis of high resolution simulations: application to turbulent plume dynamics and current sheet formation. *New Journal of Physics*, 9(8):301, 2007. URL http://stacks.iop.org/1367-2630/9/i=8/a=301.

[18] S. Servidio, W. H. Matthaeus, M. A. Shay, P. Dmitruk, P. A. Cassak, and M. Wan. Statistics of magnetic reconnection in two-dimensional magnetohydrodynamic turbulence. *Physics of Plasmas*, 17(3):032315, 2010. doi: http://dx.doi.org/10.1063/1.3368798. URL http://scitation.aip.org/content/aip/journal/pop/17/3/10.1063/1.3368798.

[19] P. Dmitruk and W. H. Matthaeus. Test particle acceleration in three-dimensional hall mhd turbulence. *Journal of Geophysical Research: Space Physics*, 111(A12):n/a–n/a, 2006. ISSN 2156-2202. doi:10.1029/2006JA011988. URL http://dx.doi.org/10.1029/2006JA011988. A12110.

[20] John Ambrosiano, William H. Matthaeus, Melvyn L. Goldstein, and Daniel Plante. Test particle acceleration in turbulent reconnecting magnetic fields. *Journal of Geophysical Research: Space Physics*, 93(A12):14383–14400, 1988. ISSN 2156-2202. doi: 10.1029/JA093iA12p14383. URL http://dx.doi.org/10.1029/JA093iA12p14383.

[21] J. F. Drake, M. Swisdak, H. Che, and M. A. Shay. Electron acceleration from contracting magnetic islands during reconnection. *Nature*, 443(7111):553–556, October 2006. ISSN 0028-0836. URL http://dx.doi.org/10.1038/nature05116.